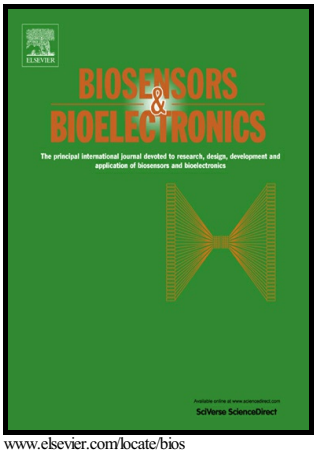

www.elsevier.com/locate/bios

Fluorescent Biosensors Enabled by Graphene and Graphene Oxide

Huan Zhang, Honglu Zhang, Ali Aldalbahi, Xiaolei Zuo, Chunhai Fan, Xianqiang Mi

PII: S0956-5663(16)30657-1
DOI: http://dx.doi.org/10.1016/j.bios.2016.07.030
Reference: BIOS8911

To appear in: *Biosensors and Bioelectronic*

Received date: 10 December 2015
Revised date: 25 June 2016
Accepted date: 7 July 2016

Cite this article as: Huan Zhang, Honglu Zhang, Ali Aldalbahi, Xiaolei Zuo Chunhai Fan and Xianqiang Mi, Fluorescent Biosensors Enabled by Graphen and Graphene Oxide, *Biosensors and Bioelectronic* http://dx.doi.org/10.1016/j.bios.2016.07.030

Fluorescent Biosensors Enabled by Graphene and Graphene Oxide

Huan Zhang[a1], Honglu Zhang[b1], Ali Aldalbahi[c], Xiaolei Zuo[b], Chunhai Fan[b], Xianqiang Mi[a*]

[a]Laboratory of System Biology, Shanghai Advanced Research Institute, Chinese Academy of Sciences, Shanghai 201210, China.

[b]Division of Physical Biology and Bioimaging Center, Shanghai Synchrotron Radiation Facility, Shanghai Institute of Applied Physics, Chinese Academy of Sciences, Shanghai 201800, China.

[c]Chemistry Department, King Saud University, P. O. Box 2455, Riyadh 11451, Saudi Arabia.

*Corresponding author, Email: mixq@sari.ac.cn

Abstract

During the past few years, graphene and graphene oxide (GO) have attracted numerous attentions for the potential applications in various fields from energy technology, biosensing to biomedicial diagnosis and therapy due to their various functionalization, high volume surface ratio, unique physical and electrical properties. Among which, graphene and graphene oxide based fluorescent biosensors enabled by their fluorescence-quenching properties have attracted great interests. The fluorescence of fluorophore or dye labeled on probes (such as melocular beacon, aptamer, DNAzymes and so on) was quenched after adsorbed on to the surface of graphene. While in the present of the targets, due to the strong interactions between probes and targets, the probes were detached from the surface of graphene, generating dramatic fluorescence, which could be used as signals for detection of the targets. This strategy was simple and economy, together with great programmable abilities of probes; we could realize detection of different kinds of species. In this review, we first briefly introduced the history of graphene and graphene oxide, and then summarized the fluorescent biosensors enabled by graphene and GO, with a detailed account of the design mechanism and comparison with other nanomaterials (e.g. carbon nanotubes and gold nanoparticles). Following that, different sensing platforms for detection of DNAs, ions, biomolecules and pathogens or cells as well as the cytotoxicity issue of graphene and GO based *in vivo* biosensing were further discussed. We hope that this review would do some help to researchers who are interested in graphene related biosening research work.

Keywords: Graphene; Graphene oxide; Biosensor; Fluorescent; Detection.

1. Introduction

Biosensors with the ability for detection of biologically active molecules are of critical importance from both biomedical, environmental, and security point of view (Lowe 1985; Scheller et al. 1991; Smith 1987; Zhu et al. 2010). Sensors usually consist of two elements: a receptor and a transducer. A receptor can be any organic or inorganic material, which can have a specific interaction with analytes. Another key element of the sensing platform is the transducer, which converts chemical information into a measurable signal. A fluorescent biosensor is a device that quantitatively or semiquantitatively converts information about the presence of a certain species to an analytically optical signal. Graphene is a single layer of graphite in which carbon atoms are arranged in a 2D hexagonal lattice. Ever since reported in 2004 (Novoselov et al. 2004), graphene has attracted a tremendous amount of interest owing to its extraordinary physicochemical and structural

[1] These authors contributed equally to this work.

properties (Geim and Novoselov 2007). While the majority of the research into the applications of graphene focuses on device fabrication, energy storage, and catalysis (Khan et al. 2015; Singh et al. 2011), graphene and its derivatives (e.g. graphene oxide, graphene quantum dots) have also emerged as a highly versatile platform for biosensor development (Liu et al. 2012b; Pumera 2011; Wang et al. 2011c; Xu et al. 2015). Graphene and graphene oxide have been implemented to construct different types of biosensors based on various sensing mechanisms, which mainly including optical/fluorescence biosensors and electrochemical sensors (Kamali et al. 2015; Liu et al. 2012b; Shao et al. 2010). According to working principle, graphene-based biosensors either use its electrical properties (e.g. high electron mobility), electrochemical properties (e. g. high electron-transfer rates), or unique structure (e.g. high surface-to-volume ratio) for biomolecule detection (Kuila et al. 2011; Zheng et al. 2014).

In this review, we will focus on fluorescent biosensors and bioanalytical systems that utilize graphene or graphene oxide as a key component. Given the vast number of works performed in this field, only selective examples are highlighted here to illustrate the design principles and strategies. We aim to provide a systematically overview of the current state of this field and hope that this may stimulate future developments.

2. Brief history of graphene and graphene oxide

Graphene is a densely packed single layer of carbon atoms, arranged in a hexagonal pattern like a honeycomb that forms a two-dimensional lattice. It can be seen as the basic building block for graphitic materials of all other dimensionalities, such as fullerenes; carbon nanotubes and graphite(Geim and Novoselov 2007) (Fig. 1A). Actually, the existence of graphene has been theoretically studied for many years (Wallace 1947) and was thought to be impossible until it was actually made by "scotch-tape" method in 2004 by Giem's group (Novoselov et al. 2004; Novoselov et al. 2005). It is reported that graphene has a large theoretical specific surface area, high electron mobility, high Young's modulus and thermal conductivity (Balandin et al. 2008; Bolotin et al. 2008; Morozov et al. 2008). Meanwhile, its high optical transmittance (~ 97.7%) and good conductivity made it excellent candidate for fabrication of transparent conductive electrodes as well as many other potential applications in electronic devices (Cai et al. 2009; Li et al. 2009). The pristine synthesis method of graphene is mechanical exfoliation, which can produce the best quality of graphene in terms of structural integrity (Zhang et al. 2005). However, this technique is only limited for scientific research due to its uncontrollable, thus large scale production and applications are limited. Another method is epitaxial growth by conversion of SiC to graphene via sublimation of silicon atoms at high temperature, which has the potential for large scale integration of nanoelectronic devices (de Heer et al. 2007). However, this method requires ultrahigh vacuum and high temperature, which may limit the accessibility due to its high cost. In recent years, a lot of research has been done for large-scale preparation of graphene using chemical vapor deposition (CVD) or exfoliation of graphene oxide (GO) solutions. Among which graphene produced by CVD method was commonly used as flexible transparent conductors for organic photovoltaic cells and in field effect transistors (Zhang et al. 2013b). While the GO solution based exfoliation method becomes quite promising, particularly for large scale applications, such as composite materials, gas sensors and supercapacitors (Park and Ruoff 2009). GO is typically synthesized through so-called Hummers' method invented many years ago (Hummers and Offeman 1958) or other modified method based on it (Marcano et al. 2010) .

Generally speaking, graphite powders are first oxidized by severe chemical regent (e.g. $KMnO_4$ or H_2SO_4), and then be exfoliated in water through mechanical energy. This process was quite easy because of the interaction of water with the oxygen-containing functional groups (such as epoxide and hydroxyl) introduced during the oxidation process. Huang and coworkers (Zhang et al. 2013a) demonstrated a convenient and high yield method of preparation of uniform ultrasmall GO nanosheets based on a modified Hummers' method, where $KMnO_4$-H_2SO_4 oxidation was repeatedly used to cut large GO nanosheets into smaller GO nanosheets with different lateral size. GO can then be substantially reduced or restored to graphene network by thermal annealing or chemical reducing agents treatment, which is usually referred as reduced graphene oxide (rGO) (Park et al. 2009).

Figure 1B is a typical schematic structure illustration of GO, rGO and pristine graphene, and all together of the three are usually named as graphene-related materials. Comparing to pristine graphene, there are many oxygenated species (including carboxyl, hydroxyl, and epoxy groups) on the surface of GO. While the oxygen groups are less on the surface of rGO, because most of them are reduced. The thickness of GO or rGO is about 1 nm, which is a little thicker than graphene owning to the oxygen containing groups on their surfaces. The above description, as well as the unique properties of high surface-to-volume ratio, various designable functional groups, opens a holy new gate for graphene and graphene oxide in application of biomedicine, such as biosensing, bioimaging and drug delivery.

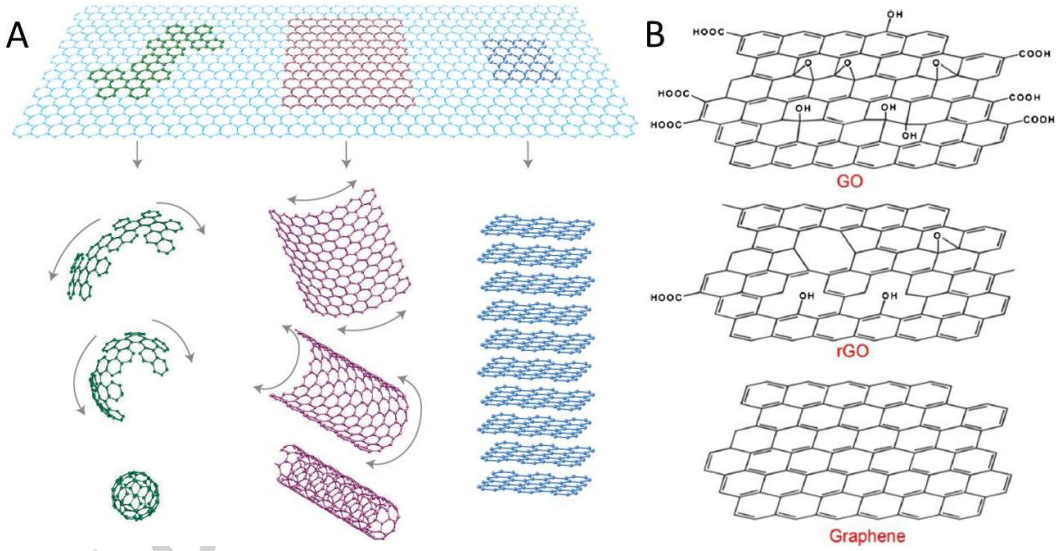

Figure 1. (A) Graphene can be wrapped up into 0D buckyballs, rolled into 1D nanotubes or stacked into 3D graphite(Geim and Novoselov 2007). (B) Schematic structures of GO, reduced GO (rGO), and pristine graphene (Liu et al. 2014c).

3, Fluorescent Biosensors based on graphene and graphene oxide (GO)

The large 2D aromatic surface structure of graphene with high ratio makes it an ideal substrate for adsorption of certain biomolecules. Actually, graphene and GO have been reported to be functionalized with nucleic acids, peptides, proteins, aptamers, small molecules, bacteria, and even cells through physical adsorption or chemical conjugation (Wang et al. 2011c). Meanwhile, it is said that graphene and GO is a general quencher, and a diverse range of species (such as fluorophores, quantum dots, and fluorescent metal

nanoclusters) can be efficiently quenched (Dong et al. 2010; Wang et al. 2011c). Theoretical calculations by Sebastian's group (Swathi and Sebastian 2008, 2009) showed that it's a long range resonance energy transfer from a dye molecule to graphene and the quenching efficiency depends on d^{-4}, where d is the distance between the fluorophore and graphene. Comparing with other molecular quenchers who usually showed a d^{-6} dependency, graphene exhibited much better fluorescence quenching ability up to a distance of 300 Å. Huang and coworkers (Kim et al. 2010) directly observed the quenching of three organic dyes by GO and rGO, and found that rGO quenches much more efficiently than GO. Further studies (Liu et al. 2011d; Matte et al. 2011) pointed out that the fluorescence quenching of the dyes by GO or graphene went through a photo-induced electron transfer process where the planar carbon π system of graphitic domains played an important role. The ability to quench all types of fluorophores with high efficiency and a wide range of functionalization makes GO or graphene a unique candidate for building fluorescent biological platforms, biosensors, and biodevices both in vitro and in vivo(Alonso-Cristobal et al. 2015; Ge et al. 2015; Liu et al. 2015a). It is important to understand the molecular mechanism and physical/chemical parameters effects to the quenching performance of GO based sensors. In this respect, several works have been done to investigate relationship of the degree of GO reduction (Hong et al. 2012a) and the length of fluorescently labeled ssDNA from GO (Huang and Liu 2012) with fluorescence quenching capability. Results indicated that shorter ssDNA was more sensitive to GO based fluorescent sensors and high C/O ratios leading to increased quenching efficiency was linked to the extent of oxidation of the nanosheets, which directly affects the area of residual graphitic domains on the sheet surface. Meanwhile, Fan's group also pointed out that the sp^2 domains in the basal plane of GO and rGO provide the main driving force for the binding of DNA to the surface of GO and rGO (He et al. 2010). Through altering the sp^2 domain of the GO, programmable biosensors with dynamic detection ranges could be designed and generated (Zhang et al. 2014). Actually, a comparative study on the quenching effects of different materials was also done by Fan's group (Li et al. 2013a), where a series of nanomaterials with different dimensions, i.e., gold nanoparticles (AuNPs, 0D), carbon nanotubes (CNTs, 1D), and graphene oxide (GO, 2D) were employed and their quenching efficiency, kinetics, differentiation ability were well studied (Figure 2A). Results showed that GO exhibited the highest quenching efficiency, fastest binding kinetics with DNA molecules, as well as best repeatability and discrimination ability for different structures of DNA (Figure 2B). To further investigate mechanisms of nanomaterial–DNA interactions, the surface area of the nanomaterials as well as the ssDNA density were measured and the surface coverage of ssDNA were calculated. They proposed that the interaction mode of DNA-Au NPs was electrostatic by Au-N interaction, while it was electrostatic π-π stacking and cation- π interaction that attributes to the interactions of ssDNA and SWNTs/GO. Moreover, the shape and the size, which offered different curvatures, were believed to be another considerable reason for the different performance of the three nanomaterials. Higher energy was consumed for the adsorbed molecules to bind to the materials with higher curvature. As we know, the 0D AuNPs has the highest curvature, then 1D SWNTs, and lastly 2D GO. Liu also pointed that DNA adsorption on AuNPs occurs via specific chemical interactions but adsorption on GO occurs via aromatic stacking and hydrophobic interactions. Meanwhile, binding induced desorption could be used for GO-based sensors while not quite suitable for AuNPs (Liu 2012).

Therefore, GO-based sensor exhibited much better performance and fluorescent biosensors based on graphene and graphene oxide nanoshhets have quite broad applications in biosensing and detection.

A

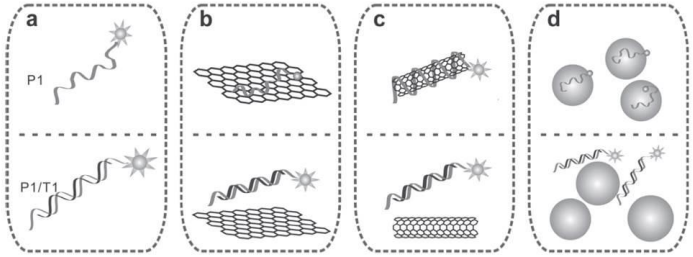

B

		GO	SWNTs	AuNPs
LOD		0.2 nM	1 nM	2 nM
SNP	F_{P1T1}/F_{P1M1}	4.1	4.5	1.9
	F_{P1T1}/F_{P1M2}	4.2	3.2	1.6
	F_{P1T1}/F_{P1M3}	3.7	5.3	1.7
RSD = SD/Mean (%)		0.5–3.8	1.5–10.4	2.3–43.4
Optimized detection time		20 s	1 min	15 min

Figure 2. (A) Scheme of several nanomaterials based DNA detection owning to their quenching property and discrimination ability of ssDNA/dsDNA. (B) Performance comparison of GO, SWNT and Au NPs-based sensors (LOD: limit of detection; SNP: single nucleotide polymorphisms, where M means single-base mismatched sequences pairs, P means probe, and T means target; RSD: relative standard deviation). (Li et al. 2013a)

3.1 *In vitro* biosening

3.1.1 DNA detection

Similar with other carbon related materials, it is not surprising that DNA can be adsorbed by graphene. We all know that the DNA bases are aromatic and so it can stack with the π electrons in graphene, just like they do with carbon nanotubes. Actually, DNA base adsorption by graphene has been studied by many researchers though computational and experimental methods (Antony and Grimme 2008; Le et al. 2012). They both came to the same conclusion of the trend G > A > C > T for DNA adsorption by density functional theory calculations (Antony and Grimme 2008) or Isothermal titration calorimetry (ITC) (Varghese et al. 2009). According to these results, graphene has emerged as a unique platform for developing DNA-based biosensors in the past few years. Chen's group (Lu et al. 2009) reported a graphene platform for sensing DNA target, where the completely quenched fluorescence of FAM-labeled ssDNA was recovered after the addition of the complementary target. They believed that in the presence of a target, the binding between the dye-labeled ssDNA and target molecule could disturb the interaction between the ssDNA and GO and alter the conformation of ssDNA to dsDNA, resulting in releasing of the dye-labeled DNA and restoration of dye fluorescence. Then Fan's group (He et al. 2010) carried out a molecular dynamics (MD) simulation to interpret large discrepancy for interactions between ss- and dsDNA with GO. They found that ssDNA were stably adsorbed by the GO and all of the nucleobases lie nearly flat at the GO surface through, while in contrast, dsDNA could not be stably adsorbed on GO in the MD simulation and retained its helical structure. To further characterize the degree of

the adsorption, they computed the distance between the atoms of the nucleobases and the surface of graphene. Results showed that the calculated distance (3.5Å) was fairly close to the van deWaals distance between a carbon atom in GO and a carbon/oxygen/nitrogen atom (the main elements of nucleobases), which suggested that most of the atoms in the nucleobases was directly adsorbed at GO. However, nucleobases of dsDNA were bonded to each other and shielded within the densely negatively charged phosphate backbone, thus hindered the adsorption. According to the findings, they demonstrated a GO-based "signal-on" DNA sensing platform, which allowed rapid, sensitive, and selective multidetection of DNA targets in homogeneous solution (Figure 3A). Liu and coworkers (Huang and Liu 2012) employed eight dual-labeled DNA molecules with varying FAM positions to control the distance between FAM and GO (Figure 3B), and found the distance for 50 % quenching was 7.5 nm. Near-complete quenching can be achieved when the fluorophore is adsorbed on the GO surface, which in turn corresponds to substantial signal enhancement upon desorption. This study further supports the feasibility of using such dye-labeled ssDNA probes for analytical and biomedical applications.

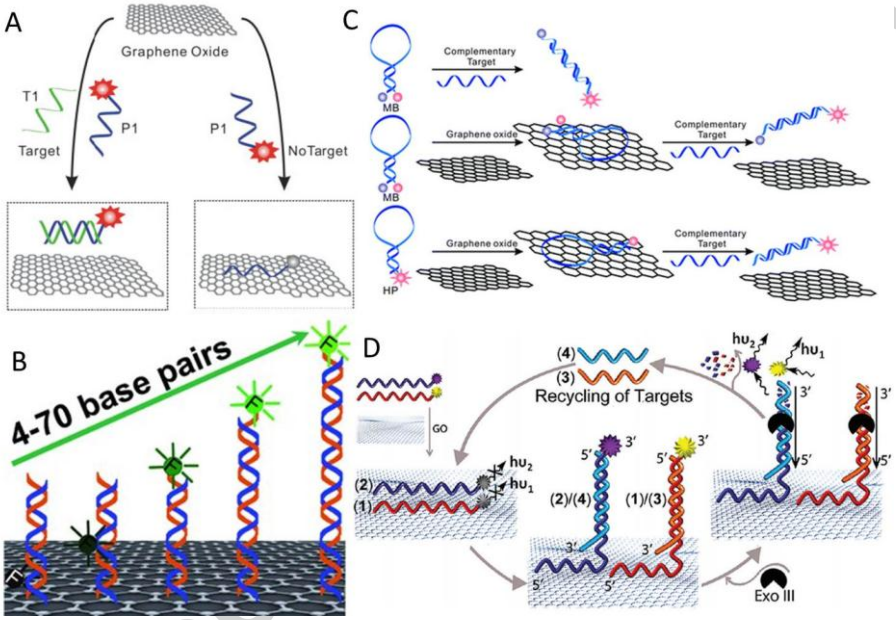

Figure 3. (A) Scheme for the fluorescent DNA detection based on the ssDNA/dsDNA discrimination ability of GO (He et al. 2010). (B) Schematic presentation of the application of DNA to control the fluorophore-to-GO distance (Huang and Liu 2012). (C) Schematic presentation of nano-MBs with GO-enhanced quenching efficiency (Li et al. 2010). The hairpin-structured DNA has stronger infinity with GO than dsDNA. (D) Amplified multiplexed analysis of DNA using graphene oxide as support and the Exo III-triggered recycling of the analytes (Liu et al. 2012a).

As the method developed, more advanced DNA-based structures and smart strategies were introduced to the system. As shown in Figure 3C, Fan and co-workers (Li et al. 2010) systematically studied the interaction between GO and MBs and found that the background fluorescence of MB was greatly decreased in the presence of GO. Then they developed a new GO-based MB probe with enhanced signal-to-background ratio, better sensitivity and higher thermal stability as compared to conventional MBs. Chen and coworkers (Lu et al. 2010a) reported a new highly sensitive, selective and economical molecular beacon probes with graphene

oxide as the "nanoquencher". Using graphene oxide greatly improved the single base-mismatch selectivity of the molecular beacon, because the conformation of the hairpin-structured oligonucleotide was constrained on the graphene oxide surface. Kim and coworkers (Yi et al. 2011) reported a system by using graphene oxide (GO) as an external quencher and realized a much higher signal-to-background ratio (31.0) relative to that (2.2) of the same system in the absence of GO.

While high sensitivity and low back ground have been realized by strong fluorescence quenching enabled by GO adsorption, further improvements was achieved by incorporating signal amplification strategies (Liu et al. 2015b). For example, Zhu's group (Zhao et al. 2012) developed a novel GO-based biosensor for DNA detection with enzymatic (exonuclease III, Exo III) based amplification. In the presence of target DNA, hybridization of probe and the target formed a double-stranded structure that had an Exo III-resistant 3 'protruding termini and a blunt 3' termini. Exo III catalyzed the stepwise removal of mononucleotides from the blunt 3' termini, releasing of the target DNA and fluorophore. The released target DNA then hybridized with another probe DNA and initiated a next round of cleavage, which produced an amplified fluorescent signal. Taking advantage of the super fluorescence quenching efficiency of GO and Exo III aided signal amplification, the sensor exhibited a high sensitivity towards target DNA with a detection limit of 20 pM, and provided a universal sensing platform for sensitive detection of various DNA. The Willner's group (Liu et al. 2012a) also reported an exonuclease-III based assay for simultaneously multiple target detection. In this case, different fluorophore-labeled probes were firstly adsorbed by GO. Then hybridization with the target DNAs led to desorption of the probes from the GO and the recovery of fluorescence to the respective label. By coupling exonuclease III to the system, the recycling of the target DNAs resulted in the amplified detection of the DNA targets with a detection limit of 5 pM, which was significantly better than the ~1 nM achieved without the signal amplification strategy (Figure 3D). Through proper design of different kind of probes, they also realized the "OR" and "AND" logic gate dictated by the color of fluorophores labeled on the probes. Li and coworkers (Yang et al. 2012) developed a new enzyme-free signal amplification-based assay for microRNA detection by using hybridization chain reaction (HCR) strategy for signal amplification with selective fluorescence quenching effects of GO. In this strategy, the target microRNAs were designed to be able to efficiently initiate HCR between two species of fluorescent hairpin probes. After HCR, the fluorescence of the hairpin probes was completely quenched by GO, while the HCR products maintained strong fluorescence, providing a simple and sensitive approach for miRNA detection in a homogeneous solution with more than 2 orders of magnitude higher sensitivity.

In summary, in this graphene or GO based DNA detection strategy, a probe with a covalently attached fluorophore is first adsorbed by GO, leading to quench of the fluorescence. When target exists, the probe is desorbed by target binding to produce a fluorescence signal. This method is attractive because of its simplicity, high signal intensity, and low background noise. It is also possible to realize multiple and more complicated detection with better performance through introducing smart design strategies.

3.1.2 Ion detection

Soft metal ions such as Ag^{+}, Pb^{2+} and Hg^{2+} can selectively bind to specific nucleobases of DNA. Some DNAzymes require certain metal ions to express their activity. DNAzyme-based sensors using many types of signal transduction mechanisms have been developed to detect a wide range

of metal ions with high selectivity and sensitivity (Zhang et al. 2011b). Among which, graphene-based metal ion sensors can be designed using DNAzymes as interfaces, which serve as both selective metal ion binder and metal-ion dependent DNA scissor for signal reporter. Fan's group (Wen et al. 2011) investigated the interactions between GO and a Pb^{2+}-dependent DNAzyme, based on which a Pb^{2+} sensor with high sensitivity, selectivity and tunable dynamic range is developed. They employed a modified version of 8-17 Pb^{2+}-dependent DNAzyme composed of an enzyme strand and a Cy3-tagged ribonucleotide-containing substrate strand, where the single ribonucleotide served as the cleavage site. In the absence of Pb^{2+}, the DNAzyme duplex rigid structure did not bind efficiently to GO, and strong emission from Cy3 was observed. While in the presence of Pb^{2+}, the substrate strand was specifically and irreversibly cleaved, resulting in the disassembly of the duplex DNAzyme into three ss-DNA fragments. The short Cy3-containing DNA piece was stably adsorbed on to the surface of GO, leading to significant quenching of the fluorescence signal, which could be used of detection of Pb^{2+} (Figure 4A). Yu and coworkers (Zhao et al. 2011) also reported a GO-DNAzyme based biosensor for amplified fluorescence "turn-on" detection of Pb^{2+}. A FAM-labeled DNAzyme substrate hybrid acted as both a molecular recognition module and the signal reporter with GO as the superquencher. By taking advantage of the super fluorescence quenching efficiency of GO, the difference in fluorescence signal intensity in the presence of Pb^{2+} versus in the absence of Pb^{2+} reached 16-fold. The proposed biosensor exhibited a high sensitivity toward the target with a detection limit of 300 pM for Pb^{2+}, which is better than those obtained using molecular dark quenchers.

A novel and promising "turn-on" fluorescent Cu^{2+} biosensor is designed by Quan's group (Liu et al. 2011a) based on graphene-DNAzyme catalytic beacon. The complex formed by the substrate strand (with the 3'-end labeled by FAM) and the Cu^{2+}-specific DNAzyme can be adsorbed by GO, leading to very low background fluorescence. While in the presence of Cu^{2+}, the substrate strand was cleaved and the FAM-labeled fragment was released, producing a fluorescence signal. Then they developed another novel and general label free fluorescent Cu (II) sensor (Liu et al. 2011b) based on internal DNA cleavage and an extrinsic fluorophore in a graphene/DNAzymes complex by using the fluorescent differences between free and intercalated GelRed. Meanwhile, the senor could realize real-time Cu (II) detection with high sensitivity and selectivity.

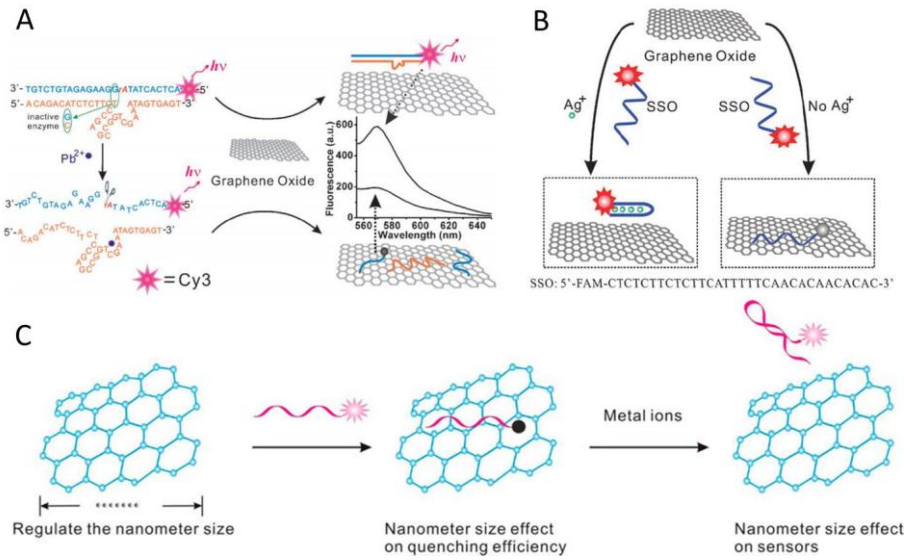

Figure 4. (A) Schematic for the Pb^{2+}-modulated interactions between DNAzyme and GO (Wen et al. 2011). (B) Schematic illustration of the fluorescence sensor for Ag(I) ions based on the target-induced conformational change of a silver specific cytosine-rich oligonucleotide (SSO) and the interactions between the fluorogenic SSO probe and graphene oxide(Wen et al. 2010). (SSO: a FAM-labeled silver-specific oligonucleotide probe). (C) Illustration of size dependent design of graphene oxide based ion sensors (Zhang et al. 2014).

It is reported (Ono et al. 2008) that specific binding of the Ag^{+} unexpectedly stabilized DNA duplexes containing the naturally occurring cytosine-cytosine (C-C) mismatch-base pair because of the C-C pair selectively binds to the Ag^{+}. The Fan group (Wen et al. 2010) developed a fluorescence sensor for Ag (I) ions based on the target-induced conformational change of a silver-specific cytosine(C)-rich oligonucleotide probe and the interactions between the probe and graphene oxide (Figure 4B). In the absence of Ag (I) ions, the FAM-labeled probe was in a flexible single strand state and adsorbed by GO, leading to fluorescence quenching. Upon addition of Ag (I) ions, the Ag (I) ions complexed with the cytosine bases and yielded a rigid hairpin structure, then the fluorescence was retained. Similarly, two thymines (T) can convergently coordinate to Hg^{2+} to form a T- Hg^{2+}-T complex hairpin structure. Fan's group also demonstrated the detection of mercuric ion (Hg^{2+}) based on a T-rich mercury specific oligonucleotide probe and graphene oxide (He et al. 2010). Without Hg^{2+}, the FAM-labeled probe was in the single stranded state and not fluorescent with GO. However, the introduction of Hg^{2+} led to the formation of the hairpin structure whose fluorescence could not be quenched by GO. The recovered fluorescence was dependent on the concentration of Hg^{2+}, and the sensor had a linear range of 30-180 nM with a detection limit of 30 nM. Then Huang and coworkers (Zhang et al. 2014) showed a dynamic range and sensitivity programmable mercury sensor based on the nanometer size effect of GO (Figure 4C). They systematically studied the nanometer size effect of GO on GO-DNA interaction, and concluded that GO of ~200 nm (lateral nanometer size) possessed the highest fluorescence quenching efficiency. By employing a FAM-labeled Hg^{2+} specific probe, three dynamic ranges (1 to 40 nM, 1 to 15 nM, and 0.1 to 5 nM) were obtained with this size modulation, and the sensitivity of Hg^{2+} was programmed from 15.3 ± 1.27 nM^{-1} to 106.2 ± 3.96 nM^{-1}.

3.1.3 Biomolecules detection

Graphene and GO-based fluorescent sensors have also been applied to detection of proteins and other biologically active small molecules. Most of these sensors used DNAs (e.g. aptamer) as an interface for both the recognition and reporting of target molecules. DNAs played the roles of a selective target binder or the substrate of enzyme, while graphene or GO was the signal transducer. The intrinsic DNA adsorption affinity difference between non-structured DNA and structured DNA were the basic design principle of these biosensors. Li's group (Chang et al. 2010) reported a graphene based fluorescence aptasensor for thrombin detection. In the work, they used a dye labeled aptamer assembled on the surface of graphene. Due to the noncovalent assembly induced by π-π stacking between DNA bases of aptamer and graphene, fluorescence resonance energy transfer (FRET) occurred from the dye to graphene, resulted in the fluorescence quenching of the dye. The addition of thrombin induced the formation of quadruplex-thrombin complexes, which have weak affinity to graphene and keep the dyes away from graphene surface, leading to recovery of the fluorescence (Figure 5A). This graphene based FRET aptasensor exhibited extraordinarily high sensitivity and excellent specificity in both buffer and blood serum with a

detection limit as low as 31.3 pM, which is two orders magnitude lower than those of fluorescent sensors based on carbon nanotubes (Yang et al. 2008). Pang's group (He et al. 2012) constructed a highly sensitive and selective fluorescent aptasensor for detection of Mucin 1 (MUC1), which is a well-known tumor biomarker. They utilized graphene oxide (GO) as a quencher to quench the fluorescence of single stranded dye-labeled MUC1 specific aptamer, while the quenched fluorescence is recovered significantly upon the adding of MUC1. This aptasensor could realize detection of MUC1 in a wide range of 0.04-10 mM with a detection limit of 28 nM. Later, they designed a novel molecular aptamer beacon (MAB) for detection of ATP by integrating a single-labeled hairpin-shaped aptamer and graphene oxide (GO). ATP can be detected in a wide range of 5-2500 μM with a detection limit of 2 μM and good selectivity.

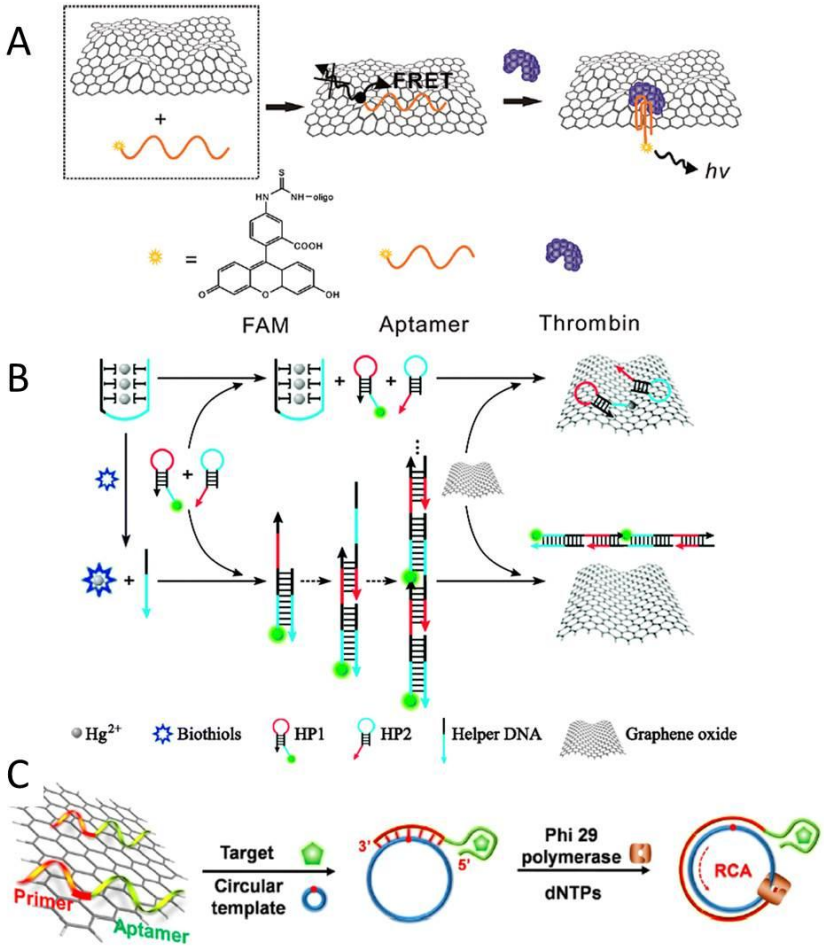

Figure 5. (A) Schematic demonstration of graphene FRET aptasensor and the detection mechanism for thrombin (Chang et al. 2010). (B) Illustration of the GO based platform coupled with hybridization chain reactions for analysis (Ge et al. 2014). (C) Schematic representation of reduced graphene oxide-aptamer-RCA biosensing platform (Liu et al. 2014a).

Recently, many elaborate sensing platforms were designed and realized ultrasensitive detections of small molecules. The Chu group (Ge et al. 2014) reported a novel fluorescent nanosensor for detecting biothiols (including cysteine and glutathione) using graphene oxide based hairpin DNA-selective fluorescence quenching and thymine-Hg(II)-thymine coordination-controlled hybridization chain reaction (HCR) signal amplification strategy. In the design, they introduced a

helper probe with a few intramolecular thymine-thymine (T-T) mismatches which can form a stem-loop hairpin structure with Hg^{2+} (T-Hg^{2+}-T coordination). In the absence of biothiols, the probe would form T-Hg^{2+}-T structure and could not induce the the HCR of fluorophore labeled HP1 and HP2. In the presence of biothiols, more stronger thiol-Hg^{2+} interactions can release the helper probe into a single stranded conformation, then it could induce the dye-labeled hairpins to form double-stranded HCR product and amplifies the fluorescence signal (as shown in Figure 5B). This novel ‘‘turn-on’’ method demonstrated superior ultrasensitivity with detection limits for cysteine and glutathione of 0.08 nM and 0.1 nM, which also increased the sensing reliability comparing to previous ‘‘turn-off’’ techniques. Li’s group (Liu et al. 2014a) designed a graphene-based ultrasensitive biosensing platform based on the release of DNA probes and rolling circle amplification (RCA) for detection of both small-molecule and macromolecular targets. The sensing platform has two important elements: the reduced graphene oxide as a transducing mediator and an ssDNA probe. The probe contained two important sequence domains: a 3’ domain that acted as the primer to initiate RCA (through the binding of a circular DNA template) and a 5’ domain made of an aptamer acted as the molecular recognition section (Figure 5C). First, the ssDNA probe was adsorbed onto the surface of reduced graphene oxide surface through π-π stacking, making it unavailable for the primer to initiate RCA. Then in the presence of the targets for the aptamer, the adsorbed probes took a target-induced conformational change that facilitated their release from the reduced graphene oxide surface, liberating the primer domain for RCA. Therefore, the detection of the target was converted to detection of the RCA products and the platform could achieve ultrasensitive detection of protein, DNA and small-molecule (e.g. the detection limit for the ATP and DNA was found to be 60 nM and 0.8 pM, respectively).

3.2 *In vivo* biosening

It is reported by Yang et.al.(Lu et al. 2010b) that functionalized nanoscale graphene oxide can protect oligonucleotides from enzymatic cleavage and efficiently deliver oligonucleotides into cells. Since then, nano-graphene has attracted tremendous interest in biomedicine (Yang et al. 2013), including bioimaging (Hong et al. 2012b; Peng et al. 2010; Sun et al. 2008), nanocarrier for drug and gene delivery (Liu et al. 2008; Wen et al. 2012; Zhang et al. 2011a; Zhang et al. 2010a), photo-induced therapy (Robinson et al. 2011; Yang et al. 2010), antibacterial (Hu et al. 2010; Zhao et al. 2013) and so on. Among which, intracellular fluorescent sensing is mainly discussed in this section. Intracellular ATP detection was well established due to the important biological function and a DNA aptamer, which has been widely used as a model system for ATP/Adenosine detection and selected by Huizenga and Szostak in 1995 (Huizenga and Szostak 1995). Lin and coworkers (Shao et al. 2010) designed an aptamer-carboxyfluorescein (FAM)/graphene oxide nanosheet (GO-nS) nanocomplex to investigate its ability for real-time monitoring of ATP in living cells. As shown in Figure 6A, ATP aptamer labeled with FAM was firstly incubated with GO-nS to form an aptamer-FAM/GO-nS sensing platform. Then the sensor was incubated with JB6 cells in culture medium, where effective cellular uptake and a fluorescence signal were observed, because of the reaction between the internalized aptamer/GO complex and ATP. The dramatic delivery, protection, and sensing capabilities of graphene oxide nanosheets in living cells were shown in this system, make it a robust candidate for use in many biological fields. Later on, they constructed another sensing platform based on this strategy for simultaneous visualization of ATP and GTP in live cells by employing two aptamers (Wang et al. 2013).

Based on the above mentioned study, Li's group (Wang et al. 2014) presented a detailed protocol for in situ multiple fluorescence monitoring of adenosine-5'-triphosphate (ATP) and guanosine-5'-triphosphate (GTP) in MCF-7 breast cancer cells by using graphene oxide nanosheet (GO-nS) and DNA/RNA aptamers. FAM-labeled ATP aptamer and Cy5-modified GTP aptamer were designed to construct the multiple aptamer/GO-nS sensing platform through "π-π stacking" between aptamers and GO-nS, which resulted in the "fluorescence off" of the aptamers caused by fluorescence resonance energy transfer from fluorophores to GO-nS. When the aptamer/GO-nS were internalized inside the cells via endocytosis, the conformation of the aptamers would change their conformations due to interactions with cellular ATP and GTP. On the basis of the fluorescence "off/on" switching, multiple sensing and imaging of ATP and GTP in vitro and in situ monitoring could be realized through fluorescence and confocal microscopy techniques (Figure 6B). Tan and coworkers (Tan et al. 2012) developed an interesting imaging method for semiquantitation of intracellular ATP molecules based on GO. They employed an ATP aptamer molecular beacon (AAMB) and a control ssDNA as internal reference, and the ATP level could be semi-quantified by using the fluorescence intensity ratio of the AAMB to the control.

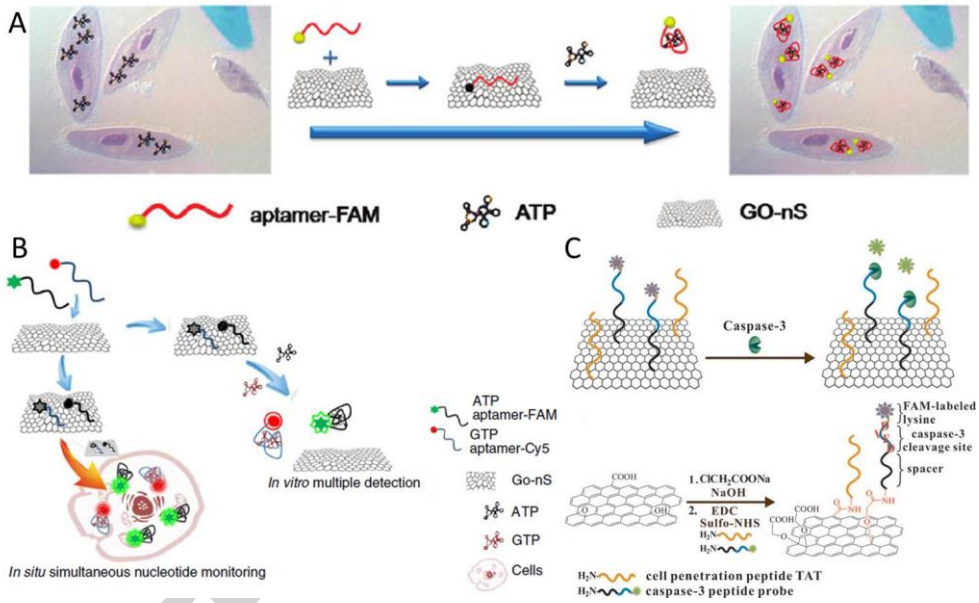

Figure 6. (A) Schematic illustration of in situ molecular probing in living cells by using aptamer/GO-nS nanocomplex (Shao et al. 2010). (B) Schematic illustration of in vitro and in situ molecular probing in living cells by using the aptamer/GO-nS nanocomplex (Wang et al. 2014). (C) Schematic representation of Caspase-3 detection using GO-peptide conjugate (top) and the construction of GO-peptide conjugate (down) (Wang et al. 2011a).

Besides ATP, other intracellular factor were also examined or monitored by graphene based fluorescent sensors. Wang and coworkers (Wang et al. 2011a) developed a sensitive, simple, and robust intracellular protease sensor for Caspase-3 activation imaging in live cells, where a FAM-labeled peptide with a caspase-3 cleavage sequence and the cell penetration peptide were covalently modified to GO surface. After being transported into cells followed by cleavage of the peptide by intracellular proteases, the GO-peptide conjugates provided significantly enhanced fluorescence signal as a result of the release of fluorophores from the GO surface (Figure 6C).

Fu's group (Li et al. 2013b) fabricated a duplex-triplex switchable DNA nanomachine for the demonstration of intracellular acidification and apoptosis of Ramos cells, where graphene oxide (GO) was employed not only as transporter but also as fluorescence quencher. This sensor could monitor the change in pH occurred inside Ramos cells during apoptosis through the different adsorption affinities of ssDNA and triplex DNA.

3.3 Detection of pathogens and cells

Detection of pathogens (such as virus, Escherichia coli) or circulating tumour cells (CTCs) is of great importance primarily for medical health diagnostics, food safety screening, and environmental pollution monitoring, where graphene or GO based fluorescent sensing platform also found its own way in this area. Liu's group (Wang et al. 2011b) reported a GO-based bioassay using a conjugated oligomer as the water-soluble neutral probe for light-up detection of Concanavalin A (ConA) and Escherichia coli (E. coli). As reported (Justice et al. 2006), E. coli was covered with tiny fingerlike projections containing an amino acid-sugar complex called lectin, where the sugar groups with strong affinity toward lectin were widely used for E. coli detection, such as α –mannose. As shown in Figure 7A, a fluorophore-labeled conjugated oligomer named FBT having a high density of α -mannose side chains were employed in the system, which were found to show very strong π-π interaction with GO. By virtue of the fluorescence quenching capability of GO, the fluorescence of the probe was low due to the fluorescence resonance energy transfer (FRET). While in the present of the ConA, the probe would preferentially bind with ConA, which would hinder the FRET and ultimately led to efficient fluorescence recovery. The newly designed sensor could realize visual detection of ConA or E. coli with high sensitivity and selectivity.

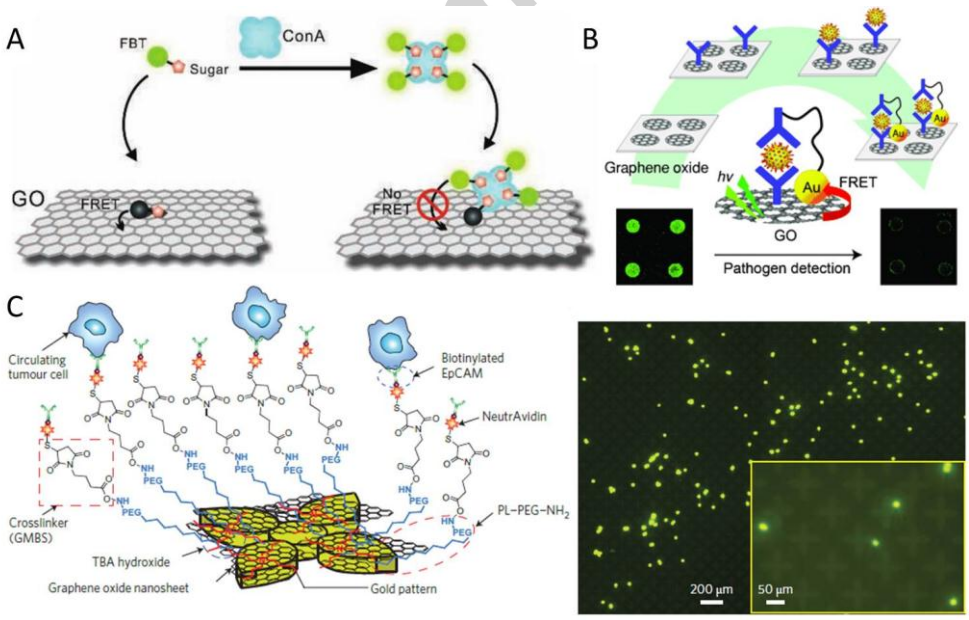

Figure 7. (A) The principle of ConA detection with the GO/FBT hybrid probe (Wang et al. 2011b). (B) A GO-based immuno-biosensor system for detection of a rotavirus as a pathogen model (Jung et al. 2010). (C) Schematic showing graphene oxide nanosheets mediated functionalization of EpCAM antibodies on the gold pattern (left) and Fluorescence image of the captured MCF-7 cells (right) (Yoon et al. 2013).

Graphene based fluorescent microarrays were also designed for detection of virus and cells. Seo and coworkers (Jung et al. 2010) exhibited a GO-based immuno-biosensor array for pathogen detection, where a rotavirus-specific antibody was chemically linked via -NH_2 groups to -COOH groups present on graphene oxide. After binding of the rotavirus to a chemically attached antibody, a secondary antibody linked to gold nanoparticles (AuNPs) was added as a label. The detection was realized induced by fluorescence resonance energy transfer (FRET) between GO sheets and AuNPs, using GO as the energy donor (Figure 7B). This immune pathogen sensor with high selectivity, sensitivity (~1000 pfu ml^{-1}) and rapid detection time could be a promising alternative to the conventional time-consuming pathogen detection methods. The Nagrath group (Yoon et al. 2013) reported a platform for sensitive capture of circulating tumour cells (CTCs) by functionalized graphene oxide nanosheets. As we all known, CTCs were detached from the primary tumour and moved from the bloodstream to a new site of subsequent tumour growth, who carried information about the primary tumour and thus had great potential to be valuable biomarkers for diagnosis and progression monitoring of the tumour (Bauernhofer et al. 2005; Cristofanilli 2006; Cristofanilli et al. 2004). However, the sensitivity and specificity of current methods for measuring and studying these cells in patient blood samples still needed to be improved. As shown in Figure 7C, the chip array presented here by Nagrath's group (Yoon et al. 2013) took advantage of functionalized graphene oxide nanosheets for sensitive capture of CTCs on a flat substrate. Firstly, graphene oxide nanosheets were adsorbed onto the patterned gold surface, and then were non-covalently functionalized by phospholipid-polyethylene-glyco-amine (PL-PEG-NH2) and Tetrabutylammonium (TBA), where TBA cations and the hydrophobic lipid chains of PL-PEG-NH2 were strongly immobilized onto the graphene oxide surface by electrostatic attraction (Wang et al. 2009a). After that, N-g-maleimidobutyryloxy succinimide ester (GMBS) was introduced, which has N-hydroxysuccinimide (NHS) esters that can react with the amine groups of the graphene oxide-PEG to form amide bonds. The CTCs could be captured by subsequent NeutrAvidin and biotinylated EpCAM antibody interactions. The novel strategy that uses graphene oxide for sensitive planar CTC capture showed higher capture yields and detection sensitivities for single-digit CTCs spiked into blood were much than the previous work (Wang et al. 2009b). Moreover, the graphene oxide chip successfully isolates CTCs from early-stage lung cancer patients as well as advanced metastatic cancer patients, which would greatly benefit for early cancer detection.

4, Cytotoxicity of graphene and graphene oxide

Given the exceptional promise of biomedical applications for graphene and its derivatives (e.g., graphene oxide, GO) mentioned above, the potential impact of them on human and environmental health has raised considerable concerns. Generally speaking, carbon-based nanomaterials are regarded as "safe" since the carbon element is inherently compatible with living systems. However, a range of carbon nanomaterials, including carbon nanutubes, nanodiamond graphene oxide have been studied to exhibit little cytotoxicity in living cell lines (Chang et al. 2011; Zhang et al. 2012; Zhang et al. 2010b). As to graphene and GO, a concentration- and time-dependent manner was observed after exposure to graphene or GO, which was attributed to the generation of reactive oxygen, indicating an oxidative stress mechanism of the cytotoxicity. It was also found out that GO or rGO have abtibacterial abilities arising from the effects of either oxidative stress or physical disruption of the bacterials, while shows little toxicity towards cells, which is quite

confusing. (Hu et al. 2010; Liu et al. 2011c; Tu et al. 2013). Further studies showed that the cytotoxicity were close related to their physical perperties (such as size, fabrication method, and oxygen content/surface charge, funtionalization) as well as the incubation environment with living cells (Chng and Pumera 2015; Liu et al. 2008; Zhang et al. 2010a). As donmenstrated by Fan's group (Zhang et al. 2013a), the prepared uniform ultrasmall GO nanosheets showed excellent biocompatibility of lower cytotoxicity and higher cellular uptake amount compared to the random large GO nanosheets (Figure 8B). Results from Dai's group also indicated that nanosized graphene oxide exhibited little toxicity and could be used as effcient carrier for biomedine applications (Liu et al. 2008; Robinson et al. 2011; Yang et al. 2013). As we can see in Figure 8A, the cytotoxicity of GO nanosheets arised from direct interactions between the cell membrane and GO nanosheets, which resulted in physical damage to the cell membrane. However, this effect is largely attenuated when GO was first incubated with FBS. Because it would form a protein-coated GO owning to its extremely high protein adsorption ability (Hu et al. 2011). Recent studies by Zhou's group (Duan et al. 2015) verified that protein BSA coating could mitigate the cytotoxicity of GO by reducing its cell membrane penetration throuth both experimental and theoretical approaches, which provide new insights into the underlying molecular mechanism of the toxicity of grphene related nanomaterials. On the other side, the physical properties of graphene or GO could be tuned as well as funtionalized with other biocimpatible molecules to reduce the cytoxicity, and thus granteened their bioligical applications.

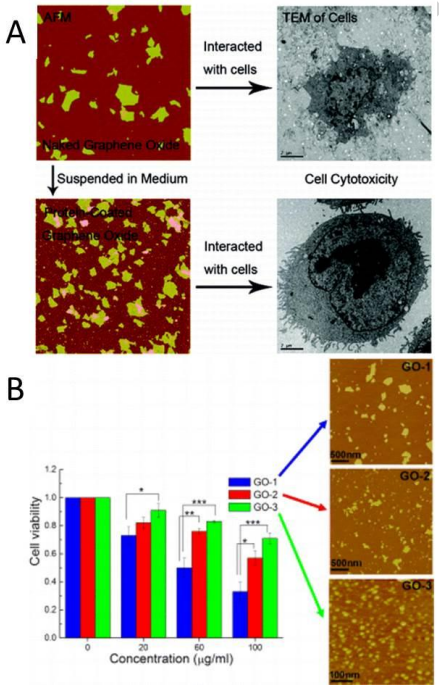

Figure 8. (A) AFM characterization of naked GO sheets and protein- coated GO (left); TEM characterization of the morphology of cells incubated with different GO nanosheets (right) (Hu et al. 2011). (B) Cytotoxicity of different sized GO nanoshhets evaluated by MTT assay (Zhang et al. 2013a).

5, Summary and future perspectives

In this review, we summarized the fluorescent sensors based on graphene and graphene oxide, which demonstrated broad applications for both *in vitro* and *in vivo* biodetection (Liu et al. 2014b;

Wang et al. 2011c). Impressive progress has already been made in the detection of environmental and biomedical targets such as DNA, RNA and metal ions et al. It is even possible to realize detection in living cells or detection of pathogens or CTCs with the help of bioarray or biochip. Even with these achievements, there are still problems needed to be overcome before this technology can reach its full potential, which also pointed out the future directions of research in this field. First, it is important to demonstrate real applications for biosensor development and an inevitable step for them to reach the next stage. Although detection in live cells has been achieved, most of the current sensors employed fluorophore-labeled probes to absorbed on the surface of graphene or GO. While under this situation, the stability of the platform, the nonspecific absorption of other substrates and the probe release are problems that must be dealt with. Second, the cytotoxicity of graphene and graphene oxide (Hu et al. 2011; Zhang et al. 2013a) must be carefully considered, such as the lateral size, the oxygen content and the dose used. We hope that towards our systematically overview of this field, more inspired design and solutions could be found in the future research work.

Acknowledgement

This work was supported by Science and Technology Commission of Shanghai Municipality (Grant 13DZ1940200 and 15441905000), Chinese Academy of Sciences (Grant KFJ-EW-STS -140, KFJ-EW-STS-096), and Shanghai Yang Fan Plan (Grant 15YF1413300). Ali Aldalbahi acknowledged Distinguished Scientist Fellowship Program of King Saud University.

References

Alonso-Cristobal, P., Vilea, P., El-Sagheer, A., Lopez-Cabarcos, E., Brown, T., Muskens, O.L., Rubio-Retama, J., Kanaras, A.G., 2015. Acs Appl Mater Inter 7(23), 12422-12429.

Antony, J., Grimme, S., 2008. Phys. Chem. Chem. Phys. 10(19), 2722-2729.

Balandin, A.A., Ghosh, S., Bao, W.Z., Calizo, I., Teweldebrhan, D., Miao, F., Lau, C.N., 2008. Nano Lett. 8(3), 902-907.

Bauernhofer, T., Zenahlik, S., Hofmann, G., Balic, M., Resel, M., Pirchmoser, R., Regitnig, P., Ambros, P., Dandachi, N., Samonigg, H., 2005. Oncol. Rep. 13(2), 179-184.

Bolotin, K.I., Sikes, K.J., Jiang, Z., Klima, M., Fudenberg, G., Hone, J., Kim, P., Stormer, H.L., 2008. Solid State Commun. 146(9-10), 351-355.

Cai, W.W., Zhu, Y.W., Li, X.S., Piner, R.D., Ruoff, R.S., 2009. Appl. Phys. Lett. 95(12), 123115

Chang, H.X., Tang, L.H., Wang, Y., Jiang, J.H., Li, J.H., 2010. Anal. Chem. 82(6), 2341-2346.

Chang, Y.L., Yang, S.T., Liu, J.H., Dong, E., Wang, Y.W., Cao, A.N., Liu, Y.F., Wang, H.F., 2011. Toxicol Lett 200(3), 201-210.

Chng, E.L.K., Pumera, M., 2015. 5(4), 3074-3080.

Cristofanilli, M., 2006. Semin. Oncol. 33(3), S9-S14.

Cristofanilli, M., Budd, G.T., Ellis, M.J., Stopeck, A., Matera, J., Miller, M.C., Reuben, J.M., Doyle, G.V., Allard, W.J., Terstappen, L.W.M.M., Hayes, D.F., 2004. New. Engl. J. Med. 351(8), 781-791.

de Heer, W.A., Berger, C., Wu, X.S., First, P.N., Conrad, E.H., Li, X.B., Li, T.B., Sprinkle, M., Hass, J., Sadowski, M.L., Potemski, M., Martinez, G., 2007. Solid State Commun. 143(1-2), 92-100.

Dong, H.F., Gao, W.C., Yan, F., Ji, H.X., Ju, H.X., 2010. Anal. Chem. 82(13), 5511-5517.

Duan, G.X., Kang, S.G., Tian, X., Garate, J.A., Zhao, L., Ge, C.C., Zhou, R.H., 2015. Nanoscale 7(37), 15214-15224.

Ge, J., Huang, Z.M., Xi, Q., Yu, R.Q., Jiang, J.H., Chu, X., 2014. Chem. Commun. 50(80), 11879-11882.

Ge, S.G., Lan, F.F., Yu, F., Yu, J.H., 2015. New J Chem 39(4), 2380-2395.

Geim, A.K., Novoselov, K.S., 2007. Nat. Mater. 6(3), 183-191.

He, S., Song, B., Li, D., Zhu, C., Qi, W., Wen, Y., Wang, L., Song, S., Fang, H., Fan, C., 2010. Adv. Funct. Mater. 20(3), 453-459.

He, Y., Lin, Y., Tang, H.W., Pang, D.W., 2012. Nanoscale 4(6), 2054-2059.

Hong, B.J., An, Z., Compton, O.C., Nguyen, S.T., 2012a. Small 8(16), 2469-2476.

Hong, H., Yang, K., Zhang, Y., Engle, J.W., Feng, L., Yang, Y., Nayak, T.R., Goel, S., Bean, J., Theuer, C.P., Barnhart, T.E., Liu, Z., Cai, W., 2012b. Acs Nano 6(3), 2361-2370.

Hu, W., Peng, C., Luo, W., Lv, M., Li, X., Li, D., Huang, Q., Fan, C., 2010. Acs Nano 4(7), 4317-4323.

Hu, W., Peng, C., Lv, M., Li, X., Zhang, Y., Chen, N., Fan, C., Huang, Q., 2011. Acs Nano 5(5), 3693-3700.

Huang, P.J.J., Liu, J.W., 2012. Small 8(7), 977-983.

Huizenga, D.E., Szostak, J.W., 1995. Biochemistry 34(2), 656-665.

Hummers, W.S., Offeman, R.E., 1958. J. Am. Chem. Soc. 80(6), 1339-1339.

Jung, J.H., Cheon, D.S., Liu, F., Lee, K.B., Seo, T.S., 2010. Angew. Chem. Int. Ed 49(33), 5708-5711.

Justice, S.S., Hunstad, D.A., Seed, P.C., Hultgren, S.J., 2006. P. Natl. Acad. Sci. USA 103(52), 19884-19889.

Kamali, K.Z., Pandikumar, A., Sivaraman, G., Lim, H.N., Wren, S.P., Sun, T., Huang, N.M., 2015. Rsc Adv 5(23), 17809-17816.

Khan, M., Tahir, M.N., Adil, S.F., Khan, H.U., Siddiqui, M.R.H., Al-warthan, A.A., Tremel, W., 2015. J Mater Chem A 3(37), 18753-18808.

Kim, J., Cote, L.J., Kim, F., Huang, J.X., 2010. J. Am. Chem. Soc. 132(1), 260-267.

Kuila, T., Bose, S., Khanra, P., Mishra, A.K., Kim, N.H., Lee, J.H., 2011. Biosens. Bioelectron. 26(12), 4637-4648.

Le, D., Kara, A., Schroder, E., Hyldgaard, P., Rahman, T.S., 2012. J Phys-Condens. Mat. 24(42).

Li, F., Huang, Y., Yang, Q., Zhong, Z., Li, D., Wang, L., Song, S., Fan, C., 2010. Nanoscale 2(6), 1021-1026.

Li, F., Pei, H., Wang, L.H., Lu, J.X., Gao, J.M., Jiang, B.W., Zhao, X.C., Fan, C.H., 2013a. Adv Funct Mater 23(33), 4140-4148.

Li, X.M., Song, J., Cheng, T., Fu, P.Y., 2013b. Anal. Bioanal. Chem. 405(18), 5993-5999.

Li, X.S., Zhu, Y.W., Cai, W.W., Borysiak, M., Han, B.Y., Chen, D., Piner, R.D., Colombo, L., Ruoff, R.S., 2009. Nano Lett. 9(12), 4359-4363.

Liu, J.Q., Liu, Z., Barrow, C.J., Yang, W.R., 2015a. Anal Chim Acta 859, 1-19.

Liu, J.W., 2012. Phys Chem Chem Phys 14(30), 10485-10496.

Liu, M., Song, J.P., Shuang, S.M., Dong, C., Brennan, J.D., Li, Y.F., 2014a. Acs Nano 8(6), 5564-5573.

Liu, M., Zhang, W.Q., Chang, D.R., Zhang, Q., Brennan, J.D., Li, Y.F., 2015b. Trac-Trend Anal Chem 74, 120-129.

Liu, M., Zhao, H., Chen, S., Yu, H., Zhang, Y., Quan, X., 2011a. Biosens. Bioelectro. 26(10), 4111-4116.

Liu, M., Zhao, H.M., Chen, S., Yu, H.T., Zhang, Y.B., Quan, X., 2011b. Chem. Commun. 47(27), 7749-7751.

Liu, S.B., Zeng, T.H., Hofmann, M., Burcombe, E., Wei, J., Jiang, R.R., Kong, J., Chen, Y., 2011c. Acs Nano 5(9), 6971-6980.

Liu, X.Q., Aizen, R., Freeman, R., Yehezkeli, O., Willner, I., 2012a. Acs Nano 6(4), 3553-3563.

Liu, Y., Liu, C.Y., Liu, Y., 2011d. Appl. Surf. Sci. 257(13), 5513-5518.

Liu, Y.X., Dong, X.C., Chen, P., 2012b. Chem. Soc. Rev. 41(6), 2283-2307.

Liu, Z., Liu, B., Ding, J., Liu, J., 2014b. Anal. Bioanal. Chem. 406(27), 1618-2642.

Liu, Z., Robinson, J.T., Sun, X.M., Dai, H.J., 2008. J. Am. Chem. Soc. 130(33), 10876-10877.

Liu, Z.B., Liu, B.W., Ding, J.S., Liu, J.W., 2014c. Anal. Bioanal. Chem. 406(27), 6885-6902.

Lowe, C.R., 1985. Biosensors 1(1), 3-16.

Lu, C.H., Li, J., Liu, J.J., Yang, H.H., Chen, X., Chen, G.N., 2010a. Chem-Eur J. 16(16), 4889-4894.

Lu, C.H., Yang, H.H., Zhu, C.L., Chen, X., Chen, G.N., 2009. Angew. Chem. Int. Ed 48(26), 4785-4787.

Lu, C.H., Zhu, C.L., Li, J., Liu, J.J., Chen, X., Yang, H.H., 2010b. Chem. Commun. 46(18), 3116-3118.

Marcano, D.C., Kosynkin, D.V., Berlin, J.M., Sinitskii, A., Sun, Z.Z., Slesarev, A., Alemany, L.B., Lu, W., Tour, J.M., 2010. Acs Nano 4(8), 4806-4814.

Matte, H.S.S.R., Subrahmanyam, K.S., Rao, K.V., George, S.J., Rao, C.N.R., 2011. Chem. Phys. Lett. 506(4-6), 260-264.

Morozov, S.V., Novoselov, K.S., Katsnelson, M.I., Schedin, F., Elias, D.C., Jaszczak, J.A., Geim, A.K., 2008. Phys. Rev. Lett. 100(1).

Novoselov, K.S., Geim, A.K., Morozov, S.V., Jiang, D., Zhang, Y., Dubonos, S.V., Grigorieva, I.V., Firsov, A.A., 2004. Science 306(5696), 666-669.

Novoselov, K.S., Jiang, D., Schedin, F., Booth, T.J., Khotkevich, V.V., Morozov, S.V., Geim, A.K., 2005. P. Natl. Acad. Sci. USA 102(30), 10451-10453.

Ono, A., Cao, S., Togashi, H., Tashiro, M., Fujimoto, T., Machinami, T., Oda, S., Miyake, Y., Okamoto, I., Tanaka, Y., 2008. Chem. Commun.(39), 4825-4827.

Park, S., An, J., Jung, I., Piner, R.D., An, S.J., Li, X., Velamakanni, A., Ruoff, R.S., 2009. Nano Lett. 9(4), 1593-1597.

Park, S., Ruoff, R.S., 2009. Nat. Nanotechnol. 4(4), 217-224.

Peng, C., Hu, W., Zhou, Y., Fan, C., Huang, Q., 2010. Small 6(15), 1686-1692.

Pumera, M., 2011. Mater. Today 14(7-8), 308-315.

Robinson, J.T., Tabakman, S.M., Liang, Y., Wang, H., Sanchez Casalongue, H., Vinh, D., Dai, H., 2011. J. Am. Chem. Soc. 133(17), 6825-6831.

Scheller, F.W., Hintsche, R., Pfeiffer, D., Schubert, F., Riedel, K., Kindervater, R., 1991. Sensor. Actuat B-Chem. 4(1-2), 197-206.

Shao, Y.Y., Wang, J., Wu, H., Liu, J., Aksay, I.A., Lin, Y.H., 2010. Electroanal. 22(10), 1027-1036.

Singh, V., Joung, D., Zhai, L., Das, S., Khondaker, S.I., Seal, S., 2011. Prog. Mater. Sci. 56(8), 1178-1271.

Smith, M., 1987. Nature 329(6138), 402-402.

Sun, X.M., Liu, Z., Welsher, K., Robinson, J.T., Goodwin, A., Zaric, S., Dai, H.J., 2008. Nano Res. 1(3), 203-212.

Swathi, R.S., Sebastian, K.L., 2008. J. Chem. Phys. 129(5), 054703.

Swathi, R.S., Sebastian, K.L., 2009. J. Chem. Phys. 130(8), 086101.

Tan, X.H., Chen, T., Xiong, X.L., Mao, Y., Zhu, G.Z., Yasun, E., Li, C.M., Zhu, Z., Tan, W.H., 2012. Anal. Chem. 84(20), 8622-8627.

Tu, Y.S., Lv, M., Xiu, P., Huynh, T., Zhang, M., Castelli, M., Liu, Z.R., Huang, Q., Fan, C.H., Fang, H.P., Zhou, R.H., 2013. Nat. Nanotechnol. 8(8), 594-601.

Varghese, N., Mogera, U., Govindaraj, A., Das, A., Maiti, P.K., Sood, A.K., Rao, C.N.R., 2009. Chemphyschem 10(1), 206-210.

Wallace, P.R., 1947. Phys. Rev. 71(7), 476-476.

Wang, H., Zhang, Q., Chu, X., Chen, T., Ge, J., Yu, R., 2011a. Angew. Chem. Int. Ed 50(31), 7065-7069.

Wang, H.L., Wang, X.R., Li, X.L., Dai, H.J., 2009a. Nano Res. 2(4), 336-342.

Wang, L., Pu, K.-Y., Li, J., Qi, X., Li, H., Zhang, H., Fan, C., Liu, B., 2011b. Adv. Mater. 23(38), 4386-4391.

Wang, S.T., Wang, H., Jiao, J., Chen, K.J., Owens, G.E., Kamei, K.I., Sun, J., Sherman, D.J., Behrenbruch, C.P., Wu, H., Tseng, H.R., 2009b. Angew. Chem. Int. Ed 48(47), 8970-8973.

Wang, Y., Li, Z.H., Wang, J., Li, J.H., Lin, Y.H., 2011c. Trends. Biotechnol. 29(5), 205-212.

Wang, Y., Li, Z.H., Weber, T.J., Hu, D.H., Lin, C.T., Li, J.H., Lin, Y.H., 2013. Anal. Chem. 85(14), 6775-6782.

Wang, Y., Tang, L.H., Li, Z.H., Lin, Y.H., Li, J.H., 2014. Nat. Protoc. 9(8), 1944-1955.

Wen, H., Dong, C., Dong, H., Shen, A., Xia, W., Cai, X., Song, Y., Li, X., Li, Y., Shi, D., 2012. Small, n/a-n/a.

Wen, Y., Xing, F., He, S., Song, S., Wang, L., Long, Y., Li, D., Fan, C., 2010. Chem. Commun. 46(15), 2596-2598.

Wen, Y.Q., Peng, C., Li, D., Zhuo, L., He, S.J., Wang, L.H., Huang, Q., Xu, Q.H., Fan, C.H., 2011. Chem. Commun. 47(22), 6278-6280.

Xu, F.Z., Shi, H., He, X.X., Wang, K.M., He, D.G., Yan, L., Ye, X.S., Tang, J.L., Shangguan, J.F., Luo, L., 2015. Analyst 140(12), 3925-3928.

Yang, K., Feng, L.Z., Shi, X.Z., Liu, Z., 2013. Chem. Soc. Rev. 42(2), 530-547.

Yang, K., Zhang, S., Zhang, G., Sun, X., Lee, S.-T., Liu, Z., 2010. Nano Lett. 10(9), 3318-3323.

Yang, L., Liu, C.H., Ren, W., Li, Z.P., 2012. ACS Appl. Mat. Interfaces 4(12), 6450-6453.

Yang, R.H., Tang, Z.W., Yan, J.L., Kang, H.Z., Kim, Y.M., Zhu, Z., Tan, W.H., 2008. Anal. Chem. 80(19), 7408-7413.

Yi, J.W., Park, J., Singh, N.J., Lee, I.J., Kim, K.S., Kim, B.H., 2011. Bioorg. Med. Chem. Lett. 21(2), 704-706.

Yoon, H.J., Kim, T.H., Zhang, Z., Azizi, E., Pham, T.M., Paoletti, C., Lin, J., Ramnath, N., Wicha, M.S., Hayes, D.F., Simeone, D.M., Nagrath, S., 2013. Nat. Nanotechnol. 8(10), 735-741.

Zhang, H., Jia, S., Lv, M., Shi, J., Zuo, X., Su, S., Wang, L., Huang, W., Fan, C., Huang, Q., 2014. Anal. Chem. 86(8), 4047-4051.

Zhang, H., Peng, C., Yang, J., Lv, M., Liu, R., He, D., Fan, C., Huang, Q., 2013a. ACS Appl. Mat. Interfaces 5(5), 1761-1767.

Zhang, L.M., Lu, Z.X., Zhao, Q.H., Huang, J., Shen, H., Zhang, Z.J., 2011a. Small 7(4), 460-464.

Zhang, L.M., Xia, J.G., Zhao, Q.H., Liu, L.W., Zhang, Z.J., 2010a. Small 6(4), 537-544.

Zhang, X.B., Kong, R.M., Lu, Y., 2011b. Annu. Rev. Anal. Chem. 4, 105-128.

Zhang, X.Y., Hu, W.B., Li, J., Tao, L., Wei, Y., 2012. Toxicol Res-Uk 1(1), 62-68.

Zhang, Y., Zhang, L.Y., Zhou, C.W., 2013b. Acc. Chem. Res. 46(10), 2329-2339.

Zhang, Y.B., Ali, S.F., Dervishi, E., Xu, Y., Li, Z.R., Casciano, D., Biris, A.S., 2010b. Acs Nano 4(6), 3181-3186.

Zhang, Y.B., Tan, Y.W., Stormer, H.L., Kim, P., 2005. Nature 438(7065), 201-204.

Zhao, J., Deng, B., Lv, M., Li, J., Zhang, Y., Jiang, H., Peng, C., Li, J., Shi, J., Huang, Q., Fan, C., 2013. Adv. Healthcare Mater. 2(9), 1259-1266.

Zhao, X.H., Kong, R.M., Zhang, X.B., Meng, H.M., Liu, W.N., Tan, W., Shen, G.L., Yu, R.Q., 2011. Anal. Chem. 83(13), 5062-5066.

Zhao, X.H., Ma, Q.J., Wu, X.X., Zhu, X., 2012. Anal. Chim. Acta. 727, 67-70.

Zheng, Q., Wu, H., Wang, N., Yan, R., Ma, Y.H., Guang, W.J., Wang, J.Z., Ding, K.J., 2014. Curr. Nanosci. 10(5), 627-637.

Zhu, Y.W., Murali, S., Cai, W.W., Li, X.S., Suk, J.W., Potts, J.R., Ruoff, R.S., 2010. Adv. Mater. 22(35), 3906-3924.

Highlights:

- Bioanalytical systems that utilize graphene or graphene oxide as a key transducer component draw great attentions of many researchers.
- Graphene and graphene oxide are unique candidates for building fluorescent biological platforms, biosensors, and biodevices both in vitro and in vivo.
- Fluorescent biosensors enabled by graphene and graphene oxide are quite attractive because of the simplicity, high signal intensity, and low background noise.